Momentum Distribution Sum Rule for Angle-Resolved Photoemission

doi: 10.1103/PhysRevLett.74.4951

Momentum Distribution Sum Rule for Angle-Resolved Photoemission

Mohit Randeria,[1] Hong Ding,[1,2] J-C. Campuzano,[1,2] A. Bellman,[1,3] G. Jennings,[1] T. Yokoya,[4] T. Takahashi,[4] H. Katayama-Yoshida,[4] T. Mochiku,[5] and K. Kadowaki[5]

[1]*Materials Sciences Division, Argonne National Laboratory, Argonne, Illinois 60439*
[2]*Department of Physics, University of Illinois at Chicago, Chicago, Illinois 60680*
[3]*Department of Physics, University of Milan, Milan, Italy*
[4]*Department of Physics, Tohoku University, 980 Sendai, Japan*
[5]*National Research Institute for Metals, Sengen, Tsukuba, Ibaraki 305, Japan*
(Received 29 December 1994)

Within a spectral function $A(\mathbf{k},\omega)$ interpretation of angle-resolved photoemission (ARPES), the intensity obeys the sum rule $\int d\omega\, f(\omega)A(\mathbf{k},\omega) = n(\mathbf{k})$, where f is the Fermi function and $n(\mathbf{k})$ the momentum distribution. We show the usefulness of this sum rule for analyzing ARPES data. The integrated intensity in $Bi_2Sr_2CaCu_2O_8$ *at* $\mathbf{k}_F$ is independent of temperature even though the spectrum is strongly T dependent. We also demonstrate the possibility of measuring $n(\mathbf{k})$ using ARPES for $YBa_2Cu_4O_8$.

PACS numbers: 79.60.–i, 74.25.Jb, 74.72.–h

Angle-resolved photoemission spectroscopy (ARPES) has played a major role in the study of the high temperature superconductors (HTSC). Some of the important results obtained by ARPES are a Luttinger Fermi surface in the normal state [1,2], flat bands or extended saddle-point singularities in the band structure [3,4], and observation of the superconducting gap [5] and its anisotropy [6,7]. These results are largely deduced from the positions of spectral features; the next set of important questions require an understanding of spectral line shapes.

Formally, photoemission measures a nonlinear response function given by a three current correlation [8]. Under certain simplifying conditions, principally the validity of the impulse approximation, this reduces to a much simpler result [9] involving only the one-particle spectral function $A(\mathbf{k},\omega)$. For a quasi-two-dimensional system, one then finds that the ARPES intensity $I(\mathbf{k},\omega) \propto f(\omega)A(\mathbf{k},\omega)$, where f is the Fermi function. With 20–30 eV incident photons, it is not *a priori* obvious that these simplifications should be justified.

Our aim here is to assume the spectral function interpretation, deduce some general consequences, and check them experimentally with a minimum of additional assumptions and without making fits involving free parameters. The success of this strategy, as described below, greatly strengthens the case for a simple $A(\mathbf{k},\omega)$ interpretation for ARPES spectra.

More specifically, we explore the consequences of a well-known sum rule relating the integrated ARPES intensity to the momentum distribution. Somewhat surprisingly, the usefulness of this sum rule has been overlooked in the ARPES literature. Our main results are as follows: (1) At $\mathbf{k} = \mathbf{k}_F$ we derive an approximate sum rule which explains why the area under the ARPES curves for $Bi_2Sr_2CaCu_2O_8$(BISCO) is essentially independent of temperature, even though the line shapes themselves have strong T dependence. (2) Based on our analysis we conclude that the observed sharpening of the ARPES peak in the superconducting state is *not* a pileup in the density of states. It is, in fact, a consequence of the sum rule together with the dramatic increase in the single-particle lifetime below T_c, presumably due to electron-electron interactions. (3) We demonstrate the possibility of measuring the momentum distribution $n(\mathbf{k})$ using energy-integrated ARPES signals for $YBa_2Cu_4O_8$. Note that $n(\mathbf{k})$ is a quantity of great theoretical interest and its experimental determination is very important.

We begin with some standard formalism to introduce our notation. The one-particle spectral function $A(\mathbf{k},\omega) = -(1/\pi)\,\mathrm{Im}G(\mathbf{k},\omega + i0^+)$ can be written as the sum of two pieces $A(\mathbf{k},\omega) = A_-(\mathbf{k},\omega) + A_+(\mathbf{k},\omega)$. In terms of exact eigenstates $|m\rangle$ with energy $\mathcal{E}_m$, the spectral weight to add a particle to the system is given by $A_+(\mathbf{k},\omega) = Z^{-1}\sum_{m,n} e^{-\beta\mathcal{E}_m}|\langle n|c_{\mathbf{k}}^\dagger|m\rangle|^2\delta(\omega + \mathcal{E}_m - \mathcal{E}_n)$, and the spectral weight to extract a particle from the system $A_-(\mathbf{k},\omega) = Z^{-1}\sum_{m,n} e^{-\beta\mathcal{E}_m}|\langle n|c_{\mathbf{k}}|m\rangle|^2\delta(\omega + \mathcal{E}_n - \mathcal{E}_m)$, where Z is the partition function and $\beta = 1/T$. It follows from these definitions that $A_-(\mathbf{k},\omega) = f(\omega)A(\mathbf{k},\omega)$ and $A_+(\mathbf{k},\omega) = [1 - f(\omega)] \times A(\mathbf{k},\omega)$, where $f(\omega) = 1/[\exp(\beta\omega) + 1]$ is the Fermi function.

Since an ARPES experiment involves removing an electron from the system, within a simple golden rule calculation the measured intensity is proportional to $A_-(\mathbf{k},\omega)$:

$$I(\mathbf{k},\omega) = I_0(\mathbf{k})f(\omega)A(\mathbf{k},\omega)\,. \tag{1}$$

The prefactor I_0 has $\mathbf{k}$ dependence from the electron-photon matrix element $|M|^2$. The dependence of I_0 on the incident photon energy and polarization, and on the final state, is not explicitly shown above. The important point

is that I_0 does *not* have any significant ω or T dependence. Thus the line shape of the energy distribution curve (EDC) and its T dependence are completely characterized by the spectral function and the Fermi factor.

We now discuss various sum rules for $A(\mathbf{k}, \omega)$ and their possible relevance to photoemission [10]. The simplest one, $\int_{-\infty}^{+\infty} d\omega\, A(\mathbf{k}, \omega) = 1$, is not useful for ARPES since it involves both occupied *and unoccupied* states, i.e., it is a sum rule for photoemission (A_-) plus inverse photoemission (A_+). Next, the one-particle density of states (DOS) is given by $\sum_{\mathbf{k}} A(\mathbf{k}, \omega) = N(\omega)$, and thus, ignoring the $\mathbf{k}$ dependence of the prefactor I_0, the well-known sum rule for the conservation of states in the DOS would apply to *angle-integrated* photoemission [11]. However, provided one has sharp momentum resolution one is *not* summing over all $\mathbf{k}$'s, and the commonly used description of the sharpening of the ARPES peak below T_c as the "BCS pileup in the DOS" is simply not correct. The correct interpretation will be discussed below.

The important sum rule for ARPES is

$$\int_{-\infty}^{+\infty} d\omega\, f(\omega) A(\mathbf{k}, \omega) = n(\mathbf{k}), \qquad (2)$$

which directly relates the energy-integrated ARPES intensity to the momentum distribution $n(\mathbf{k}) = \langle c_{\mathbf{k}}^{\dagger} c_{\mathbf{k}} \rangle$. (The sum over spins is omitted for simplicity.)

Let us use the notation "$\mathbf{k} = \mathbf{k}_F$" to denote $\mathbf{k}$ on the Fermi surface for a normal system. For a superconductor, we use $\mathbf{k} = \mathbf{k}_F$ to denote $\mathbf{k}$ such that the excitation energy is a minimum with respect to $|\mathbf{k}|$ for a fixed $\hat{\mathbf{k}}$. Experimentally, for BISCO is has been shown that $\mathbf{k}_F$ in the normal and superconducting states coincide [7].

Recall that $n(\mathbf{k}_F) = \frac{1}{2}$ is independent of T for the free Fermi gas and the BCS superconductor (and also in Eliashberg theory [12]). In all of these cases this result follows from "particle-hole symmetry": $A(-\epsilon_{\mathbf{k}}, -\omega) = A(\epsilon_{\mathbf{k}}, \omega)$. We will argue that, under more general conditions, $n(\mathbf{k}_F)$, and hence the integrated intensity *at* $\mathbf{k}_F$, is independent of T above and below T_c. We can rewrite Eq. (2) as $n(\mathbf{k}) = \frac{1}{2} - \int_0^{\infty} d\omega \tanh(\beta\omega/2)[A(\mathbf{k}, \omega) - A(\mathbf{k}, -\omega)]/2$. Thus $n(\mathbf{k}_F)$ is *independent of temperature* provided $A(\mathbf{k}_F, -\omega) = A(\mathbf{k}_F, \omega)$; in fact, the latter condition is required only for low frequencies [13]. We emphasize the approximate nature of the $\mathbf{k}_F$ sum rule since there is no exact symmetry which enforces it.

Note that only for $\mathbf{k} = \mathbf{k}_F$ is $n(\mathbf{k})$ T independent. [For $\mathbf{k}$'s far from $\mathbf{k}_F$ with excitation energies much larger than T, we expect no T dependence in $n(\mathbf{k})$ either.] However, for $\mathbf{k}$ near $\mathbf{k}_F$ we expect qualitatively different T dependences for occupied and unoccupied states. For increasing T, in the normal state, $n(\mathbf{k})$ should decrease for $\mathbf{k}$ inside the Fermi surface while it should increase for $\mathbf{k}$ outside.

In Fig. 1(a) we show EDC's for BISCO ($T_c = 87$ K) on the Fermi surface along the $\bar{M}Y$ direction [at point 1 in the Brillouin zone (BZ) in Fig. 1], for $95 \geq T \geq 13$ K.

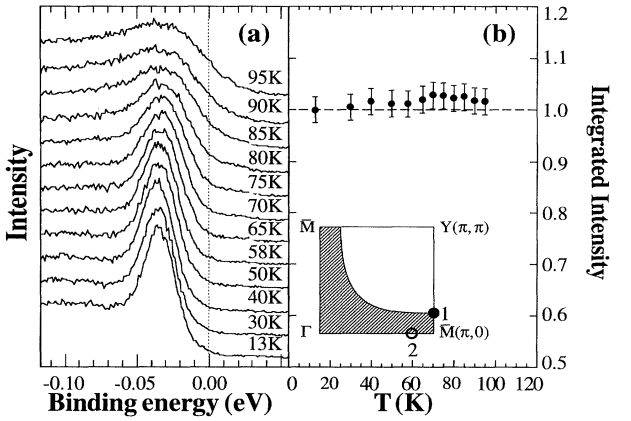

FIG. 1. (a) ARPES spectra for BISCO at $\mathbf{k} = \mathbf{k}_F$ (point 1 in the BZ shown in inset) for various temperatures; the base lines are shifted for clarity. (b) Integrated intensity as a function of temperature for the data shown in (a).

Details of the experimental procedure and on the samples may be found in Ref. [7]. The optically flat sample surface quality is crucial for the observation [7] of sharp peaks with substantial dispersion. The energy resolution for the data in Fig. 1 is a Gaussian with $\sigma = 8$ meV (FWHM $\simeq 19$ meV) and the momentum resolution is $\pm 1°$. We note that the very sharp energy resolution is not essential for our present purposes since we will be interested in energy-integrated quantities here. However, sharp momentum resolution is of the essence.

An important point in comparing data at different temperatures is the normalization of the EDC's. The data were recorded in absolute units: number of electrons per incident photon. However, the sample surface loses adsorbed gases with increasing T, leading to small T-dependent increases in intensity. To account for this, and changes in the position of the sample due to thermal expansion of the holder, a small adjustment (<5% for freshly cleaved samples) was made in the normalization using the following criterion. Data at a fixed $\mathbf{k}$ but different T were normalized so that the positive binding energy background (flat part at $\omega > 40$ meV which is unrelated to the signal of interest, primarily at $\omega < 0$) is the same for all T. After normalization the $\omega > 0$ background was chosen to be the common zero base line.

In Fig. 1(b) we plot the integrated intensity of the EDC's as a function of T and find that, in spite of the remarkable changes in the line shape from 95 to 13 K [see Fig. 2(a)], the integrated intensity at $\mathbf{k}_F$ is very weakly T dependent. The error bars come from the normalization due to the low count rate in the $\omega > 0$ background. Similar results are obtained at other points on the Fermi surface.

The T-dependent changes in the line shape may be understood as follows. At 95 K one has a very broad

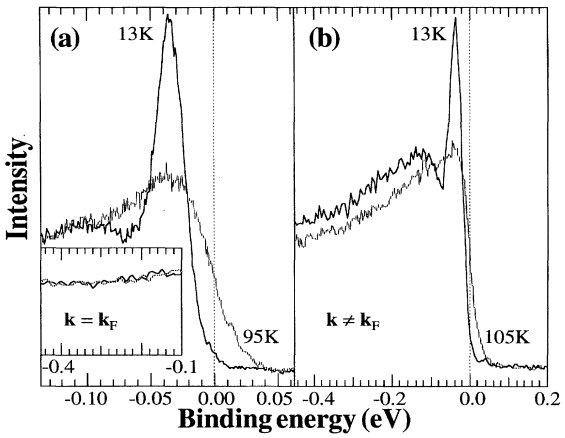

FIG. 2. (a) Selected data from Fig. 1(a) plotted to show the change in line shape and the matching of intensities beyond -100 meV. Inset: lower resolution data up to higher binding energies. (b) Lower energy resolution data away from $\mathbf{k}_F$ (at point 2 in the BZ of Fig. 1) to show the lack of matching at large binding energy.

$A(\mathbf{k}_F, \omega)$, with a maximum at $\omega = 0$, which is cut off by the Fermi function. For $T < T_c$ a gap begins to open up and spectral weight shifts down to negative energies $\omega = -|\Delta(\mathbf{k})|$. See Ref. [7] for a detailed analysis of the 13 K data along these lines. Another striking feature of the data is the sharpening of the peak with decreasing T. This indicates that the scattering rate Γ of the quasiparticles, which determines the linewidth of $A(\mathbf{k}, \omega)$, drops sharply in the superconducting state in qualitative agreement with analysis of optical and microwave data [14]. The quantitative extraction of the frequency and temperature dependence of this lifetime will be taken up in a later publication. Finally, note that with decreasing linewidth the sum rule can only be satisfied with a large increase in the peak intensity. This then is not a DOS pileup, but rather a consequence of the strong T dependence of Γ, presumably due to electron-electron interactions, as the gap opens up.

The T independence of the integrated intensity is insensitive to the choice of the integration cutoff at negative ω, provided it is chosen beyond the dip feature (whose origin is not clear at present). As seen from Fig. 2(a) and inset, the normalized EDC's at $\mathbf{k}_F$ have identical intensities for $\omega < -100$ meV. This is quite reasonable, since we expect the spectral functions be the same for energies much larger than the scale associated with superconductivity. The fact that one has to go to 100 meV in order to satisfy the sum rule suggests that electron-electron interactions are involved in superconductivity.

Let us now discuss the integrated intensity away from $\mathbf{k}_F$. In Fig. 2(b) we plot the data for point 2 in the BZ in Fig. 1. Unlike the data at $\mathbf{k}_F$ in Fig. 2(a) we find that the spectral functions above and below T_c do not agree at large binding energies. Since changes in $A(\mathbf{k}, \omega)$ down to 400 meV cannot be expected to arise from superconductivity with $T_c = 87$ K, there must be a T-dependent "background" contribution. Note that this background has T dependence away from $\mathbf{k}_F$ [Fig. 2(b)] but not at $\mathbf{k}_F$ [Fig. 2(a)], consistent with data from other groups [5]. Remarkably, this is precisely described by a phenomenological model of secondary emission of inelastically scattered electrons in which the background is modeled as $C \int_\omega^\infty d\epsilon\, I(\mathbf{k}, \epsilon)$. Thus the background has the same T dependence as the integrated intensity. Subtracting out this background with a suitably chosen C, we find that the integrated intensity decreases by about 10% when T is raised from 13 to 105 K. The details of this analysis will be presented elsewhere, together with a critical discussion of the background modeling. A proper understanding of the background is crucial for making detailed fits to the line shape [15]. However, we must emphasize that a background of the form described above does not affect our sum rule analysis *at* $\mathbf{k}_F$.

Finally, an important application of the $n(\mathbf{k})$ sum rule would be to use it to experimentally determine the momentum distribution itself. In view of the above discussion of background subtraction, it is useful to illustrate this idea on $YBa_2Cu_4O_8$ (Y124) where the signal is greatly enhanced [3] (for an incident photon energy of 28 eV), and thus the background can be safely ignored. This can be seen from the EDC's shown in Fig. 3 (see, e.g., curve labeled 8). Details of the samples and the experiments were presented earlier [3]. It must be mentioned, however, that ARPES on Y124 find no evidence for superconductivity, presumably due to problems with the disruption of the surface layer upon cleaving. (In contrast, BISCO has a van der Waals coupled BiO bilayer where it cleaves.) Thus the data presented for Y124 (bulk $T_c = 82$ K) will be in a nonsuperconducting state at 12 K; we shall determine the

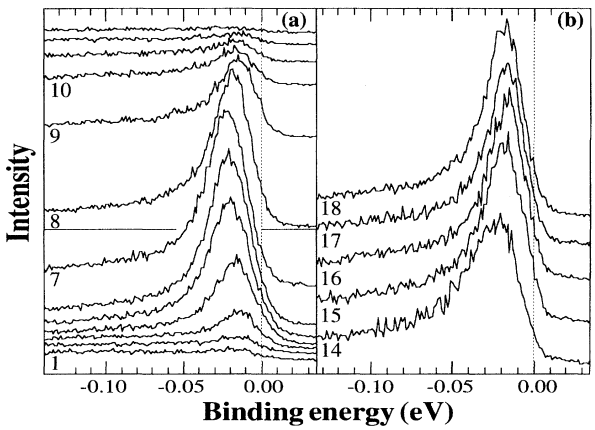

FIG. 3. EDC's for $YBa_2Cu_4O_8$ at 12 K for various $\mathbf{k}$'s. (a) Spectra 1 through 13 are along the S-Y-S direction shown in the BZ in Fig. 4, and (b) Spectra 14 through 18 are along ΓY.

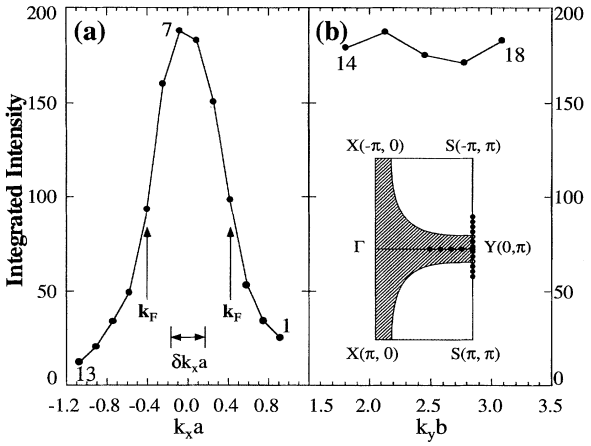

FIG. 4. Integrated intensity, which is proportional to $n(\mathbf{k})$, for the EDC's in Fig. 3, as a function of $\mathbf{k}$ for points marked in the BZ. The arrows show the Fermi surface crossings inferred from Fig. 3.

momentum distribution of this normal state by integrating the EDC's over the energy interval shown in Fig. 3.

The integrated intensity is plotted along two directions in the BZ in Fig. 4. We get information about $n(\mathbf{k})$ only to the extent that we can assume the prefactor $I_0(\mathbf{k})$ in Eq. (1) to be constant in the small range of $\mathbf{k}$'s of interest. (It is possible to improve upon this by obtaining matrix elements from electronic structure calculations, especially since experiments show that matrix elements for equivalent points in two zones can be very different.)

The momentum density peaks at the bottom of the band at the Y $(0, \pi)$ point and then decreases to zero along the YS (k_x) direction. The Fermi surface crossings along the S-Y-S direction deduced from the dispersion data in Fig. 3 are marked on the $n(\mathbf{k})$ plot in Fig. 4. The width of the observed $n(\mathbf{k})$ is dominated by our momentum resolution of $\pm 1°$ corresponding to $\delta k_x a \simeq \pm 0.17$ shown in Fig. 4. With improved momentum resolution, it is possible that in the future ARPES will be able to address the important question of the $T = 0$ singularity in $n(\mathbf{k})$. We note that this is the first measurement of $n(\mathbf{k})$ for the CuO plane electrons [16].

In conclusion, we present experimental evidence for a sum rule that greatly strengthens the case for a simple spectral function interpretation of ARPES data in HTSC. We show that the energy-integrated ARPES intensity offers a novel way to experimentally study the momentum distribution.

We would like to thank A. Abrikosov, R. Fehrenbacher, R. Liu, K. Matho, M. Norman, and L. Pitaevski for discussions. This work was supported by the Division of Materials Sciences, Office of BES-DOE Contract No. W-31-109-ENG-38. The Synchrotron Radiation Center is supported by NSF Grant No. DMR-9212658.

[1] C. G. Olson *et al.*, Phys. Rev. B **42**, 381 (1990).
[2] J. C. Campuzano *et al.*, Phys. Rev. Lett. **64**, 2308 (1990).
[3] K. Gofron *et al.*, J. Phys. Chem. Solids **54**, 1193 (1993); Phys. Rev. Lett. **73**, 3302 (1994).
[4] D. S. Dessau *et al.*, Phys. Rev. Lett. **71**, 2781 (1993).
[5] C. G. Olson *et al.*, Science **245**, 731 (1989).
[6] Z. X. Shen *et al.*, Phys. Rev. Lett. **70**, 1553 (1993).
[7] H. Ding *et al.*, Phys. Rev. Lett. **74**, 2784 (1995).
[8] For reviews and references, see *Photoemission in Solids I*, edited by M. Cardona and L. Ley (Springer-Verlag, Berlin, 1978); A. Leibsch, in *Festkörperprobleme XIX*, edited by J. Treusch (Vieweg, Braunschweig, 1979).
[9] See, e.g., L. Hedin and S. Lundquist, *Solid State Physics* (Academic, New York, 1969), Vol. 23, p. 1.
[10] For earlier discussions, see P. W. Anderson, Phys. Rev. B **42**, 2624 (1990); Phys. Rev. Lett. **67**, 660 (1991); D. S. Dessau *et al.*, *ibid.* **66**, 2160 (1991).
[11] J.-M. Imer *et al.*, Phys. Rev. Lett. **62**, 336 (1989).
[12] See, e.g., D. J. Scalapino, in *Superconductivity*, edited by R. D. Parks (Dekker, New York, 1969), Vol. 1, Sect. IV.
[13] That only small frequencies are involved at low temperature may be seen from $dn(\mathbf{k}_F)/d\beta = -\int_0^\infty d\omega\, \mathrm{sech}^2(\beta\omega/2)\omega[A(\omega) - A(-\omega)]/4 - \int_0^\infty d\omega \times \tanh(\beta\omega/2)[dA(\omega)/d\beta - dA(-\omega)/d\beta]/2$, where $A(\omega) = A(\mathbf{k}_F, \omega)$. The thermal factor in the first term cuts off for $\omega > T$, and the second term only requires that $A(\mathbf{k}_F, \omega) = A(\mathbf{k}_F, -\omega)$ up to frequencies for which there is significant T dependence in $A(\mathbf{k}_F, \omega)$.
[14] M. C. Nuss *et al.*, Phys. Rev. Lett. **66**, 3305 (1991); D. A. Bonn *et al.*, *ibid.* **68**, 2390 (1992).
[15] L. Z. Liu *et al.*, J. Phys. Chem. Solids **52**, 1473 (1991).
[16] In contrast, positron annihilation results for $n(\mathbf{k})$ in $YBa_2Cu_3O_7$ are restricted to the chain bands; see *Proceedings of the Workshop on the Fermiology of High-T_c Superconductors, Argonne, 1991*, edited by A. Bansil *et al.* [J. Phys. Chem. Solids **52**, 1485–1594 (1991)].